Structural distortions in rare-earth transition-metal oxide perovskites under high pressure

J.-S. Zhou

Materials Science and Engineering Program, Mechanical Engineering, University of Texas at Austin, Austin, Texas 78712, USA

Owing to their structural complexity and wide range of possible chemical combinations, perovskite oxides exhibit many technically important physical properties. Pressure is a thermodynamic parameter which is useful for tuning physical properties; however, the response of the complex crystal structure to high pressure has not been thoroughly studied and rationalized. This study focuses on *in situ* high-pressure x-ray diffraction of the orthorhombic perovskite oxides $A^{3+}B^{3+}O_3$, commonly found for the rare-earth transition-metal oxides of the RMO_3 formula. Each of the four families of RMO_3 (M = Ti, Cr, Mn, Fe) perovskites in this study all crystallize in the same orthorhombic perovskite structure with the *Pbnm* space group. The lanthanide contraction in these materials leads to varying degrees of orthorhombic distortions that are primarily associated with octahedral site rotations. The pressure-induced change of the lattice parameters demonstrates an evolution from a suppression to an enlargement of the orthorhombic distortion for substitution of the rare-earth element from R = La to Lu in RMO_3 perovskites. This unusual crossover of the lattice parameters' dependence on pressure contradict the results from first-principles calculation but can be rationalized by the intrinsic distortion of the perovskite structure.

I. INTRODUCTION

The technical importance of perovskite oxides cannot be overstated. Understanding strongly correlated phenomena found in perovskite or perovskite-related oxides, such as high-T_c superconductivity in copper oxides and colossal magnetoresistance in manganese oxides, remains a major challenge to condensed-matter theorists. The ABO_3 perovskite structure consists of a 3D network of corner shared BO_6 octahedra with the A atom in the polyhedra formed by the octahedra. There are 15 tilting systems in the perovskite family [1], with the *Pbnm* space group system being the most popular of the group. The physical properties of perovskites are extremely sensitive to octahedral-site rotations and distortions as can be seen in many perovskite systems as the rare-earth element on the A site of the material is changed. The following serve as only a few explanatory examples of the possible transitions that can occur as the extent of octahedral site rotation is varied: (1) the transition from a Pauli paramagnetic metal to a Mott insulator in the RNiO$_3$ perovskites [2,3]; (2) RTiO$_3$ undergoes an antiferromagnet to ferromagnet transition [4]; (3) RVO$_3$ displays a variety of orbital/spin ordering states [5]; (4) a dramatic change of Néel temperature in RCrO$_3$ [6]; and (5) a spin-state transition in RCoO$_3$ [7]. High pressure is a tuning parameter of the electronic structure of these oxides as seen in the pressure-induced insulator-metal transition in PrNiO$_3$ [8] and the pressure-induced spin state transition in RCoO$_3$ [9,10]. Therefore, to understand and establish structure-property relationships for perovskites at high pressures, a precise depiction of how their structure responds to such pressures is necessary. High-pressure studies can help elucidate our understanding of physical phenomena in other

fields as well, such as in geology and mineral physics where materials under high pressure in the earth's lower mantle are studied. One such material is the orthorhombic perovskite, MgSiO$_3$, where a structural study under high pressure would prove useful in understanding its structural instability and transition to a postperovskite structure [11].

It is well known that the structural stability of a perovskite ABO_3 is determined by a geometric tolerance factor $t \equiv (A\text{-}O)/\sqrt{2}(B\text{-}O)$, where A-O and B-O are the cation to oxygen bond lengths. For $t = 1$, the perovskite has a cubic structure. Distorted perovskite structures associated with a variety of octahedral tilting systems are developed in order to accommodate the bond-length mismatch for $t < 1$; the smaller the t value, the larger an orthorhombic distortion (a quantitative relationship is given below). For $t > 1$, hexagonal-polytype structures are formed, whereas ilmenite or LiNbO$_3$-type structures are stabilized for t that falls below the lower limit of the perovskite structure [12]. An early-day argument was that, under high pressure, more covalent B-O bonding is less compressible than that of more ionic A-O bonding. This difference in bond compressibility leads to a reduction of t factor under pressure [12]. With this empirical guideline for high-pressure synthesis, new perovskites like BaRuO$_3$ [13], BaIrO$_3$ [14], and BaOsO$_3$ [15], where a $t > 1$ holds at ambient conditions, were successfully synthesized. Simply applying this rule, i.e., a $dt/dP < 0$, to a category of ABO_3 compounds with $t < 1$ would lead one to predict that even more distorted perovskite structures exist under pressure. Thus, a pressure-induced transition from ilmenite to a perovskite structure is impossible given a $dt/dP < 0$. Zhao *et al.* [16] showed that the ratio of the site compressibility is inversely proportional to the ratio of site bond valence

sum, which allows one to predict structural behavior under high pressure based on structural data at ambient condition. Additionally, they predicted that $A^{3+}B^{3+}O_3$ compounds such as RFeO$_3$ would have less of a structural distortion under high pressure (i.e., $dt/dP > 0$) compared to a $dt/dP < 0$ for $A^{2+}B^{4+}O_3$ perovskites. Motivated to resolve the same issue, Xiong *et al.* [17] have obtained the pressure dependence of the structure from first-principles calculations and showed that dt/dP approaches and crosses zero from a negative value as t increases for $A^{2+}B^{4+}O_3$. An overall $dt/dP \geqslant 0$ obtained for $A^{3+}B^{3+}O_3$ perovskite structures is consistent with the argument by Zhao *et al.*

A recent high-pressure structural study on several members of the RFeO$_3$ family by Vilarinho *et al.* [18] lead to the conclusion that the tilting distortion becomes smaller under high pressure for RFeO$_3$ compounds with rare-earth ions having a large ionic radius, whereas it becomes drastically enlarged for rare-earth ions with a smaller ionic radius. The authors did not attempt to rationalize the result they reported. In retrospect, all the examples of $A^{3+}B^{3+}O_3$ perovskites considered by Zhao *et al.* displayed a low degree of orthorhombic distortion. Although each of these previous studies has allowed for some insights into the high-pressure structural behavior of perovskites, the picture is far from complete. A methodical study on the pressure dependence of structure in these materials is necessary to rectify the current knowledge of these systems. By considering four families of $R^{3+}M^{3+}O_3$ (R = rare earth, M = Ti, Cr, Mn, Fe) perovskites with the *Pbnm* space group, we have experimentally demonstrated how the orthorhombic perovskite structure responds to pressure. For perovskite structures that begin with a high degree of structural distortion, high pressure only exacerbates the distortion. For perovskite structure with low structural distortion, high pressure further lowers the structural distortion. These results cannot be reconciled with any preconceived theories or models presented in the literature thus far, but we have found that it is rooted in an intrinsic distortion of the perovskite structure that is often overlooked.

The *Pbnm* RMO$_3$ compounds form the largest family of perovskites. Their t factor varies continuously in each series of transition-metal M owing to the lanthanide contraction. Structural studies under high pressure have been performed on some of the perovskites in the RMO$_3$ family [18–33]. However, a systematic study of multiple RMO$_3$ families covering a wide range of t factors to correlate if there is a common trend of the pressure dependence of the structure has yet to be performed. Pressure effects on the crystal structure in some RMO$_3$ families is complicated by electronic structure or spin-state transitions as in RNiO$_3$ [34] and RCoO$_3$ [9,10] respectively. For this reason, we focus here on the perovskite series of M = Ti, Cr, Mn, and Fe. RMO$_3$ perovskites with these transition metals are not known to show any pressure-induced changes of their electronic structure; thus there are no complicating factors to study their crystal structure under high pressures. Although pressure does induce a spin-state transition in RFeO$_3$ at $P \sim 400$ kbar [20]; our study is limited to $P < 100$ kbar to prevent this transition from interfering with any structural observations.

II. EXPERIMENTAL DETAILS

Powder x-ray diffraction (XRD) was performed with a diamond-anvil cell; CaF$_2$ and a 4:1 mixture of methanol and ethanol were used as the pressure manometer and the pressure medium, respectively. A monocapillary collimator was applied to replace the regular collimator with double pinholes and improved the beam intensity from a 2-kW fine-focused Mo anode tube. The XRD patterns were collected on a Fuji image plate that was scanned and digitized with a Fujifilm scanner (BAS 1800 II). The diffraction patterns were integrated to a two-column data set of intensity versus 2θ with the software FIT2D. Lebail method refinement of each XRD profile was performed with the software FULLPROF; an example of the profile fitting for NdTiO$_3$ at $P = 8.7$ kbar and lattice parameters as a function of pressure for all perovskites in this study are given in the Supplemental Material (SM) [35]. The pressure dependence of cell volume of RMO$_3$ perovskites has been fit to the Birch-Murnaghan (BM) equation with $B' = 4$ (fixed).

III. RESULTS AND DISCUSSION

The orthorhombic *Pbnm* perovskite structure is a substructure of the cubic perovskite with the *Pm-3m* space group. Orthorhombic structural distortions (widely called GdFeO$_3$-type distortions) relative to the cubic structure consist of three components: i.e., a major octahedral-site rotation around the b axis of the orthorhombic cell (the tilting subsystem $a^-a^-c^0$), a minor rotation around the 001 axis (the tilting subsystem $a^0a^0c^+$), and an A-site shift from the body-center position in a cubic primary cell. A direct consequence for the octahedral-site tilting around the b axis is to shorten the lattice parameters $c/\sqrt{2}$ and a while the b axis remains more or less unchanged, leading to $a < c/\sqrt{2} < b$. The minor rotation $a^0a^0c^+$ does not change the a/b ratio or $b - a$. However, the a/b ratio is directly related to the tilting angle due to the major titling mode $a^-a^-c^0$. The octahedral-site rotations can be calculated from the lattice parameters through the relationship given by O'Keeffe and Hyde [36] if octahedra remain rigid. For a Jahn-Teller (JT) active system such as RMnO$_3$, the cooperative JT distortion places an e_g electron in the basal plane, causing the basal plane to expand. As a result, the c axis becomes much small relative to a and b, i.e., $c/\sqrt{2} < a < b$, a relationship that is always seen in this family of materials.

Another important consideration for these materials is the local structural distortion that influences lattice parameters in addition to the three components of the GdFeO$_3$ type distortion. As an example, experimental lattice parameters as a function of t factor for the RCrO$_3$ system is provided in Fig. 1. For comparison with the experimental values, a, b, and $c/\sqrt{2}$ as a function of t were simulated with the structural prediction program SPuDs with rigid octahedra in a *Pbnm* structure [37,38]. The predicted a,b, $c/\sqrt{2}$ do not cross until a smooth orthorhombic to cubic phase transition occurs at a value of t outside the range of the plot. The lattice parameters a and $c/\sqrt{2}$ as a function of t follow the SPuDs predictions reasonably well on the side of heavily distorted RCrO$_3$, i.e., for those members with a large $b-a$. The slope of $b(t)$ also agrees
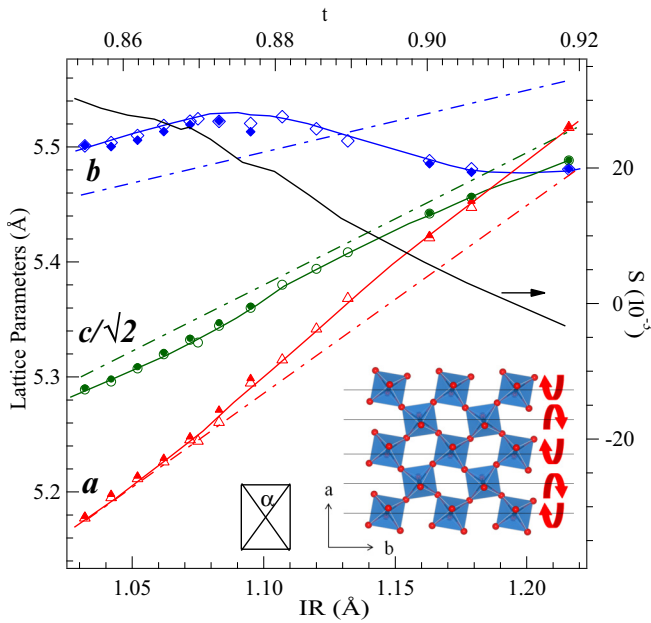
FIG. 1. The lattice parameters and the orthorhombic distortion parameter S as a function of ionic radii (IR) of rare earths (bottom x axis) or tolerance factor t (top x axis). Solid symbols represent results from neutron diffraction, hollow symbols represent results from x-ray diffraction. The dashed lines are the SPuDs simulation results. The lower right inset shows the structural model of octahedra in a-b plane; the lower middle inset shows an octahedron projected through the apical oxygen.

well with the prediction apart from a small offset between the observed b axis and the predicted b axis. This deviation from the prediction occurs at a rare-earth ionic radius (IR) ~ 1.1 Å where the observed b axis starts to decrease and the a axis increases as t increases; b eventually crosses a at some point in the orthorhombic phase, which is not allowed in the $Pbnm$ perovskite with rigid octahedra. These changes of lattice parameters as a function of t illustrated for the case of RCrO$_3$ is a universal trend for all $Pbnm$ $R^{3+}M^{3+}O_3$ perovskites with $M = 3d$ transition-metal elements [39]. The origin of the b-axis anomaly is due to the fact that the O-M-O angle α (see inset of Fig. 1 for the definition of α) in an octahedron becomes slightly less than 90° and decreases further below 90° as t increases. As a result of $\alpha < 90°$, the ab plane of the octahedra is elongated along the a axis and shortened along the b axis. This local distortion can lead to $a \approx b$ and even $a > b$. A further increase of $a - b$ is always accompanied by a first-order phase transition to the rhombohedral or the tetragonal phase as t increases (to a t out of the plot scale) by increasing temperature [40] or applying high pressure [32,41]. The SPuDs calculation predicts one smooth transition from the orthorhombic phase to the cubic phase, but in reality the orthorhombic perovskites undergo phase transitions to intermediate phases with higher symmetries than that of the $Pbnm$ structure before ending up at the cubic phase as t increases. The evolution of lattice parameters as a function of t for RCrO$_3$ offers useful guidance for deriving the change of t under pressure through the change of lattice parameters. For convenience during the remainder of this

discussion of structure under high pressure, we define a factor $S \equiv (b - a)/(b + a)$. $S(t)$ derived for the RCrO$_3$ perovskites decreases monotonically as t increases as demonstrated in Fig. 1. A reduction of $b - a$ (and therefore the S factor as a whole) reflects a decrease of the octahedral-site rotation angle in the $a^- a^- c^0$ mode. A slope change of S for IR $\geqslant 1.11$ Å is caused by local octahedral-site distortion on the lattice parameters on top of a reduced octahedral-site rotation angle. Since the general trend of lattice parameters versus t is similar for most known orthorhombic perovskites [39], the behavior of $S(t)$ should be qualitatively similar in other orthorhombic systems. Therefore, by tracking changes in S, the t factor in a perovskite becomes a measurable parameter for structural studies under pressure.

Figure 2 shows the lattice parameters' dependence on pressure for two members in the RTiO$_3$ family, NdTiO$_3$ and YbTiO$_3$. NdTiO$_3$ has a small orthorhombic distortion while YbTiO$_3$ has a much heavier distortion. These results are typical for members of other RMO$_3$ families with similar t factors to these two materials. Whereas the overall lattice parameters reduce under pressure, the b axis in NdTiO$_3$ shrinks at a steeper slope than the a axis. A reduction of S under pressure in NdTiO$_3$ indicates that t increases under pressure based on the relationship of S vs t in Fig. 1. In sharp contrast, S clearly increases under pressure in YbTiO$_3$, meaning that t decreases under pressure. There is a crossover from $dS/dP > 0$ for perovskites with a smaller IR to a $dS/dP < 0$ for those with a larger IR. The general trend for the pressure dependence of S as a function of IR is similar for each of the four systems in this study as plotted in Fig. 2 and in Figs. S2 and S6 of the Supplemental Material [35].

The LaMO$_3$ composition in each family has an S that is either negative or very close to zero at ambient pressure. Pressure causes a steeper negative slope for S, resulting in it crossing zero and into a negative value. Since the orthorhombic structure with rigid octahedra (as predicted by SPuDs) does not allow $S = 0$ or $S < 0$, the pressure effect on the orthorhombic perovskite with smaller octahedral-site rotations is to further reduce the angle α in octahedra below 90° on top of decreasing octahedral-site rotations in the structure. Hence, pressure reduces the orthorhombic distortion of the perovskite towards the cubic phase while enlarging the octahedral-site distortion away from the cubic phase. Further development of these two competitive factors under pressure always leads to a first-order phase transition. For example, LaCrO$_3$ undergoes a pressure-induced first-order structural transition from the orthorhombic $Pbnm$ phase to a rhombohedral phase $R\bar{3}$-c at $P \approx 20$ kbar; the refinement result with a two-phase model is shown in Fig. S5 of the Supplemental Material [35]. This result is consistent with previous reports in the literature [42]. This pressure-induced phase transition mimics the phase transition to a rhombohedral phase corresponding to a higher t factor and a reduced octahedral-site rotation as temperature increases above 533 K at ambient pressure [40].

The general trend of smaller S values under pressure can also be found in the RMO$_3$ (R = Pr, Nd, Sm) systems. In these materials the octahedral-site rotations are relatively small and the α deviates from 90°. For RMO$_3$ systems with further reduced IR, the S vs P curves become flat and have a weak crossover from $dS/dP < 0$ to $dS/dP > 0$.
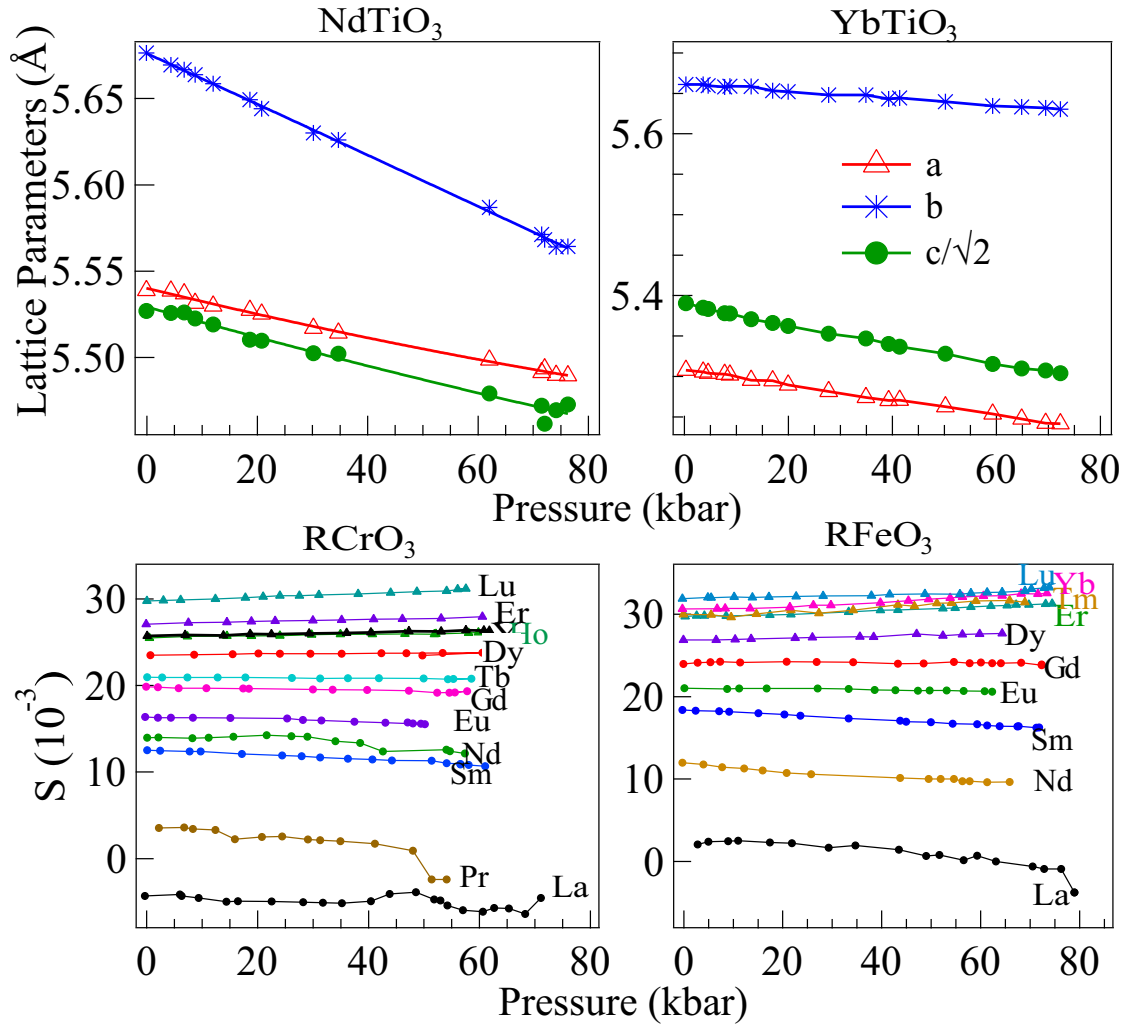
FIG. 2. Upper panels: lattice parameters as a function of pressure for two titanates, which are typical for the $R M O_3$ with larger IR (NdTiO$_3$) and the smaller IR (YbTiO$_3$). Lower panels: S factor as a function of pressure for the two families, RCrO$_3$ and RFeO$_3$. S factor as a function of pressure for the RTiO$_3$ and RMnO$_3$ families are provided in Figs. S2 and S6 [35].

Such a subtle change for perovskites having a weak pressure dependence of S becomes difficult to visualize in a plot covering a relatively large difference of S between them. Thus, for the sake of clarification, we introduce a reduced S factor, $S_r = [S(P) - S(0)]/S(0)$, shown in Fig. 3 for all four $R M O_3$ families presented in this study. The $R M O_3$ having a dramatic pressure dependence of S were omitted from this plot in order to emphasize the subtle changes near a crossover from $dS/dP < 0$ to $dS/dP > 0$. Among the JT-inactive $R M O_3$ perovskites, the crossover occurs for $R =$ Gd, Tb, Dy. In the RTiO$_3$ family, the perovskites are sharply divided into two groups with a $dS/dP < 0$ and a $dS/dP > 0$. A more continuous evolution from $dS/dP < 0$ and $dS/dP > 0$ is found for the RCrO$_3$ material family. The JT-active RMnO$_3$ shows a dramatically enlarged orthorhombic distortion owing to a cooperative JT distortion, which is reflected in a larger S than that of other JT-inactive perovskites (Fig. S6 [35]). Most members in the RMnO$_3$ family have a negative dS/dP except for LuMnO$_3$ ($dS/dP > 0$). Some members in this family, such as TmMnO$_3$, show a pressure-dependent dS/dP that is negative for lower pressures and positive for $P > 60$ kbar.
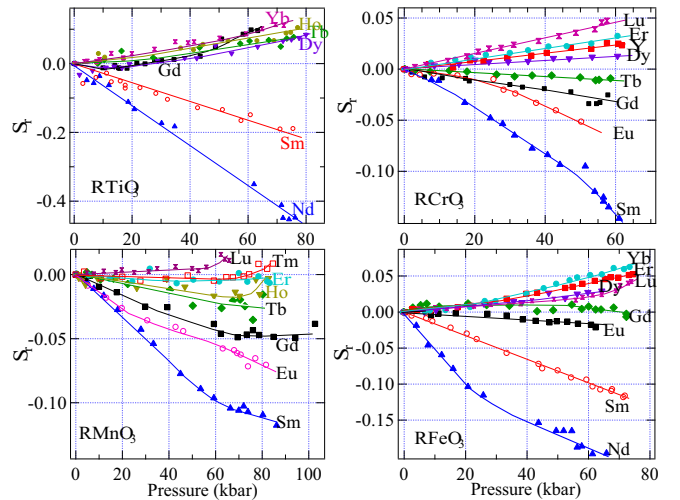

FIG. 3. The reduced S factor as a function of pressure for all four families of $R M O_3$ ($M =$ Ti, Cr, Mn, Fe).

Pressure largely favors higher symmetry crystal structures with higher density. In the orthorhombic perovskites, pressure can simply reduce the octahedral-site rotations, which consequently reduces the orthorhombic splitting described by the S factor. Pressure-induced reduction of S in RMO_3 perovskites with a relatively small octahedral-site rotation is further complicated due to the lowering of α below 90°. The effect of pressure on RMO_3 structures with IR < 1.11 Å, where α is close to 90° [39], is to reduce octahedral-site rotation. In this scenario a negative dS/dP of small magnitude is expected. If dS/dP is observed to be greater than zero, then the orthorhombic splitting and octahedral-site rotation is enlarged under pressure. These observations lead to multiple questions. How can pressure play such a sharply different role on multiple materials with the same space group within a single family of perovskites? Is it possible to account for the overall effect of pressure on JT active and JT-inactive perovskite materials?

It becomes a natural curiosity to wonder if the differences between pressure dependence of crystal structure between different perovskite materials influences their physical properties. To this end, we consider the magnetic transition of RCrO$_3$ under pressure. Mean-field theory gives a $T_N \sim J$, where J is the superexchange interaction in a Mott insulator and is proportional to the square of the orbital overlap integral based on the formula for the superexchange interaction [43]. The orbital overlap integral for the superexchange interaction in an orthorhombic perovskite is directly related to the M-O bond length and the M-O-M angle θ through the relation $\cos(180-\theta)$. Perovskites with a lower degree of octahedral-site rotation have a higher T_N. A detailed discussion of these relationships can be found elsewhere [44]. Owing to an overall reduced M-O bond length under pressure, octahedral-site rotations dictate dT_N/dP. The correlation between the structural distortion and the Néel temperature for the RCrO$_3$ perovskites has already been documented [6]. However, pressure dependence of crystal structure and its influence on the pressure dependence of T_N have not previously been explored. A dramatic increase of T_N is expected for RCrO$_3$ ($R =$ La, Pr, Nd, Sm) since the only effect of pressure is to reduce octahedral-site rotations, i.e., the Cr-O-Cr bond angle becomes closer to 180°. Conversely, octahedral-site rotations increase under pressure for the RCrO$_3$ ($R =$ Dy, Y, Er, Lu). In these cases, the pressure-induced increase of the overlap integral (basically due to shortening the Cr-O bond length) is offset by bending the Cr-O-Cr bond angle away from 180°. Therefore, we expect to see a relatively small dT_N/dP for RCrO$_3$ ($R =$ Dy, Y, Er, Lu). The experimental results of $(1/T_N)dT_N/dP = 4.3 \times 10^{-3}$ kbar^{-1} for LaCrO$_3$ [41] and $(1/T_N)dT_N/dP = 2.1 \times 10^{-3}$ kbar^{-1} for YCrO$_3$ [45] agree with these expectations very well.

To rationalize the systematic change in the pressure dependence of the structural distortion as a function of IR in each family of RMO_3, we turn to the intrinsic structural distortion of $Pbnm$ perovskites in addition to the three components of the GdFeO$_3$-type distortion. The JT effect in the $RMnO_3$ system leads to a cooperative orbital ordering in the structure and a peculiar local distortion, i.e., two long and four equally short Mn-O bonds in an MnO$_6$ octahedron, corresponding to the orbital occupation of $(3y^2 - r^2)/(3x^2 - r^2)$ alternately at neighboring Mn sites in the ab plane. This local structural distortion can be plotted in the 2D space of the orthorhombic vibration modes $Q_2 = (l_x - l_y)$ and $Q_3 = (2l_z - l_x - l_y)/\sqrt{3}$, where l_x denotes the M-O bond length, with an angle $\phi = \tan^{-1}(Q_3/Q_2)$ and a magnitude $\rho_0 = (Q_2{}^2 + Q_3{}^2)^{1/2}$. ϕ reflects how an octahedron is distorted, whereas ρ_0 is equivalent to $[\sum_{i=1-6} (l_i - l_0)^2]^{1/2}$ for the bond-length splitting of an octahedron, where l_0 is the average M-O bond length [46,47]. The orbital occupation of $(3y^2 - r^2)/(3x^2 - r^2)$ leads to a longer bond along x on one Mn site and along y for a neighboring Mn site in the a-b plane of the primary cell, which corresponds to two points on the plot (one along 120°, another along 240°). These two angles in the JT system should be independent from the orthorhombic structural distortion since the JT distortion in $RMnO_3$, i.e., two long and four equally short Mn-O bonds in an octahedron, does not depend on IR of the rare-earth element present in the material. Kanamori [48] pointed out, in a structural study of LaMnO$_3$, that the actual angle is less than 120°. This deviation indicates that there is some bias on the JT distortion by the orthorhombic structure. Zhou and Goodenough subsequently mapped out the local distortions for the entire family of $RMnO_3$ perovskites, shown in (Q_2, Q_3) space in Fig. 4 [49]. Points in the Q_2 and Q_3 space for $RMnO_3$ are mostly concentrated in two small areas far from the origin; one area is around 120° and the other is near 240°. When magnified (Fig. 4 inset) these regions reveal an evolution of the local structural distortion as a function of IR; the bond length splitting increases from La to Sm, plateaus from Gd to Tm, and slightly decreases from Tm to Lu. Remarkably, the evolution of the local distortion as a function of IR resembles that of JT-inactive systems like RFeO$_3$, also shown in Fig. 4 [44]. There are some differences between these two polar plots. The overall bond length splitting in RFeO$_3$ is smaller than that of $RMnO_3$ by about one order in magnitude. The plateau of ρ_0 for $R =$ Gd to Tm found in $RMnO_3$ is narrowed for the RFeO$_3$ system to Gd through Tb. The bond-length splitting as a function of IR may prove helpful in explaining the overall effect of pressure in perovskites.

Although lattice parameters and octahedral-site rotations change monotonically as a function of IR in an orthorhombic RMO_3 system, the local bond-length splitting (the magnitude ρ_0 in Fig. 4) exhibits a maximum near the IR of Gd. The maximum of ρ_0 separates members in each RMO_3 family into two groups with distinctly different pressure dependences of the structural distortion. To demonstrate that the structural dependence on pressure matches our classification of local structure, we will take a closer look at the compound TmFeO$_3$, which is in the middle of the wing from Gd to Lu in the plot of Fig. 4. The argument of a $dt/dP > 0$ for this material by Zhao *et al.* [16] would lead to an increase of t under pressure, i.e., pressure making TmFeO$_3$ have a structure like ErFeO$_3$ or HoFeO$_3$, both of which have a larger t. However, following this argument an increase of t under pressure can only be done at the expense of increasing local distortion, i.e., an increased ρ_0. The experimental results in Fig. 3 indicate the contrary, i.e., pressure increasing S in TmFeO$_3$ so as to lead to a structure similar to YbFeO$_3$. Ultimately, this analysis brings us to the realization that reduction of the bond-length splitting is the deciding factor for determining
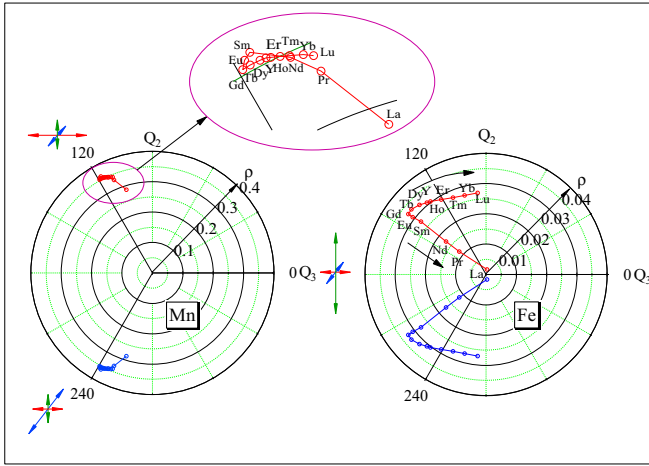
FIG. 4. Polar plot of the octahedral-site distortion in RMnO$_3$ and RFeO$_3$ orthorhombic perovskites. In the plot, an octahedron with two long bonds and four equally short bonds is located at 0° (with the long bonds along z axis), 120° (long bonds on x axis), and 240° (long bonds on y axis). An octahedron with two long bonds, two medium bonds, and two short bonds is represented by a spot at an angle between these three designated angles. Two neighboring M ions in the ab plane in the orthorhombic perovskite structure have their long bond pointing to the x axis and y axis of the primary cell, alternatively. Since the difference between the medium bond and the short bond is small, the octahedral-site distortions are described by two groups of points, one group near 120° and another near 240°. Mapping out the octahedral-site distortion for all members in the JT-inactive RFeO$_3$ indicates a continuous evolution with a maximum distortion at $R =$ Gd. Similar plots can be obtained for other JT-inactive RMO$_3$ perovskites, meaning that it is an intrinsic local distortion for the orthorhombic perovskite oxides. In the JT active RMnO$_3$ perovskites, the bond-length splitting of an octahedron increases dramatically. The structural distortions for all members are concentrated in the small areas near 120° and 240°; a magnified plot (inset) reveals an evolution of ρ_0 as a function of IR in the family.

how octahedral-site rotations change under pressure. One may ask why the structural change in TmFeO$_3$ induced by pressure does not follow the trend on the wing from Gd to La in Fig. 4, which would reduce both the octahedral-site rotation and the bond-length splitting. By following this trend under pressure, the system must go over the maximum bond-length splitting distortion near an IR of Gd, which does not appear energetically favorable. Pressure makes NdFeO$_3$ (on the wing from La to Gd) have the structure of PrFeO$_3$ or LaFeO$_3$ by reducing the bond-length splitting, corresponding to a smaller orthorhombic distortion. The same is true for other members in this wing. In summary, there are two pathways for lowering ρ_0 under pressure by following the intrinsic local distortion: (1) the wing from Gd to La where ρ_0 and the octahedral-site rotations are both reduced; (2) the wing from Gd to Lu where ρ_0 is reduced, but the octahedral-site rotations get enlarged. For the members with an IR near Gd or Tb, the structure appears to be frustrated in choosing a pathway; the octahedral-site rotations and therefore the orthorhombic distortion does not change even though the cell volume decreases under pressure. For LaCrO$_3$, the pressure-induced transition from the orthorhombic to rhombohedral phase [31,32,41,42,50–

52] results in a total elimination of the bond-length splitting in the octahedra of the rhombohedral phase required by the symmetry.

In the JT active RMnO$_3$, the JT distortion greatly enlarges the orthorhombic distortion as indicated by a significantly higher S factor in Fig. S6 [35] than that of non-JT active families. Moreover, the local distortion as described by ρ_0 of Fig. 4 is also higher [49]. The rare-earth substitution still brings about a variation of ρ_0 in the RMnO$_3$ family. Although the evolution of ρ_0 in RMnO$_3$ can be roughly separated into two wings like other non-JT active perovskite families, an obvious reduction of ρ_0 on the wing with smaller IR rare earths appears to occur in the RMnO$_3$ with R near the smallest IR shown in Fig. 4. Therefore, the pressure-induced changes for the members on this wing, i.e., reducing ρ_0 and enlarging the octahedral-site rotations, can only clearly be seen for LuMnO$_3$. For the $R =$ Gd to Tm RMnO$_3$ perovskites where ρ_0 is nearly identical across in part of the wing, the structure is frustrated under high pressure; there is relatively little change in the orthorhombic distortion under pressure.

ρ_0(IR) varies from family to family for perovskite oxides. However, the crossover from $dS/dP > 0$ to $dS/dP < 0$ is closely related to the behavior of ρ_0(IR) for each family of perovskites in this study. Therefore, it is clear that the role of high pressure on the orthorhombic perovskites is to reduce the bond-length splitting in octahedra by following the pathway of lowering ρ_0 in the polar plot of the local distortion intrinsic to the orthorhombic perovskites.

The main goal of this study is to correlate the pressure dependence of the structure with the local distortion, but a direct observation of the change of bond-length splitting under pressure remains a challenge. Pressure-induced changes of the M-O bond length are typically in the range of the error bars in most experiments, especially with laboratory x-ray diffraction because of the weak scattering of oxygen. Moreover, peak intensities are highly sensitive to the stress due to nonhydrostaticity of the medium under high pressure. This sensitivity can make it difficult to accurately refine atomic positions. A more suitable experiment for observing the trend of reducing the bond-length splitting reduction under pressure is neutron diffraction under modest pressure; the data for Cr-O bond lengths in LaCrO$_3$ is provided in Table S1 of the Supplemental Material [35,41].

This systematic study of the perovskite structure under high pressure also allows us to verify the finding by Anderson and Nafe (AN) [53]; they have shown that the bulk modulus (B_0) of a material is correlated to its cell volume, i.e., $B_0V_0 =$ const. This relation can also be derived from the interatomic potential of ionic bonds [54]. The AN rule is established for compounds with identical crystal structure, but their cell volumes spread out over a broad range, even over several orders of magnitude. The RMO$_3$ perovskites provide a test of whether the AN rule remains valid in a system in which the volume changes more continuously in a much smaller range. Figure 5 shows the B_0 vs V_0^{-1} for three families of RMO$_3$. B_0 for most perovskites fall within a narrow range of around 2000 kbar. A much lower B_0 is found in LaMnO$_3$ due to the pressure-induced change of electronic structure [33,45] Although the general trend of B_0 vs V_0^{-1} roughly follows the AN rule, there is a clear discontinuity at a unique
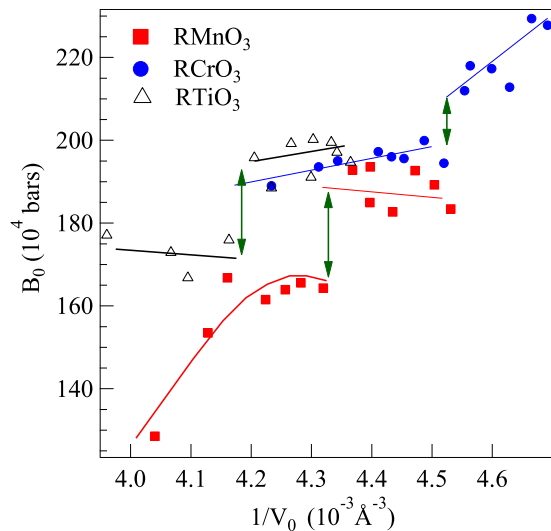
FIG. 5. The bulk modulus vs inverse cell volume for three families of RMO_3 perovskites.

cell volume for each family. It should be noted that this discontinuity occurs at a critical IR where the O-M-O bond angle α begins to deviate from 90°. This observation indicates that while the AN rule may be applicable to compounds with simple structures, the relationship of bulk modulus versus cell volume in more complex structures such as the orthorhombic perovskite does not follow the AN rule and is influenced more by local distortions.

IV. CONCLUSION

The pressure dependence of the orthorhombic distortions (PDOD) in the *Pbnm* perovskite structure has been studied for four families of rare-earth transition-metal oxides. The results indicate that the PDOD depends on the IR; it shows a general crossover from a positive to a negative PDOD as the IR increases, but the critical IR where a crossover occurs varies from family to family of perovskite oxides. The critical IR at which this crossover occurs is found to correspond to the IR where local distortion in a perovskite family is maximized. This observation leads the author to conclude that the general effect of pressure on the orthorhombic perovskites is to reduce the bond-length splitting of the octahedra in the structure. Moreover, the local structural distortion denoted by the $O_{21}-M-O_{22}$ bond angle of the octahedra influences the bulk modulus. This observation provides an example that contradicts the general rule, $B_0V_0 = const$, proposed by Anderson and Nafe.

[1] R. H. Mitchell, *Perovskites, Modern and Ancient* (Almaz, Thunder Bay, Ontario, 2002).

[2] J. B. Torrance, P. Lacorre, A. I. Nazzal, E. J. Ansaldo, and C. Niedermayer, Systematic study of insulator-metal transitions in perovskites RNiO₃ (R = Pr, Nd, Sm, Eu) due to closing of charge-transfer gap, Phys. Rev. B **45**, 8209 (1992).

[3] J. L. Garciamunoz, J. Rodriguezcarvajal, P. Lacorre, and J. B. Torrance, Neutron-diffraction study of RNiO₃ (R = La,Pr,Nd,Sm) - electronically induced structural-changes across the metal-insulator-transition, Phys. Rev. B **46**, 4414 (1992).

[4] M. Mochizuki and M. Imada, Orbital physics in the perovskite Ti oxides, New J. Phys. **6**, 154 (2004).

[5] S. Miyasaka, Y. Okimoto, M. Iwama, and Y. Tokura, Spin-orbital phase diagram of perovskite-type RVO₃ (R = rare−earth ion or Y), Phys. Rev. B **68**, 100406(R) (2003).

[6] J. S. Zhou, J. A. Alonso, V. Pomjakushin, J. B. Goodenough, Y. Ren, J. Q. Yan, and J. G. Cheng, Intrinsic structural distortion and superexchange interaction in the orthorhombic rare-earth perovskites RCrO₃, Phys. Rev. B **81**, 214115 (2010).

[7] J. Q. Yan, J. S. Zhou, and J. B. Goodenough, Bond-length fluctuations and the spin-state transition in (LCoO₃ L = La, Pr, and Nd), Phys. Rev. B **69**, 134409 (2004).

[8] J. S. Zhou, J. B. Goodenough, and B. Dabrowski, Pressure-Induced Non-Fermi-Liquid Behavior of PrNiO₃, Phys. Rev. Lett. **94**, 226602 (2005).

[9] J. S. Zhou, J. Q. Yan, and J. B. Goodenough, Bulk modulus anomaly in RCoO₃ (R = La, Pr, and Nd), Phys. Rev. B **71**, 220103(R) (2005).

[10] T. Vogt, J. A. Hriljac, N. C. Hyatt, and P. Woodward, Pressure-induced intermediate-to-low spin state transition in LaCoO₃, Phys. Rev. B **67**, 140401(R) (2003).

[11] M. Murakami, K. Hirose, K. Kawamura, N. Sata, and Y. Ohishi, Post-perovskite phase transition in MgSiO₃, Science **304**, 855 (2004).

[12] J. B. Goodenough, in *Preparative Methods in Solid State Chemistry*, edited by P. Hagenmuller (Academic, New York, 1972).

[13] C. Q. Jin, J. S. Zhou, J. B. Goodenough, Q. Q. Liu, J. G. Zhao, L. X. Yang, Y. Yu, R. C. Yu, T. Katsura, A. Shatskiy, and E. Ito, High-pressure synthesis of the cubic perovskite BaRuO₃ and evolution of ferromagnetism in ARuO(3) (A = Ca, Sr, Ba) ruthenates, Proc. Natl. Acad. Sci. USA **105**, 7115 (2008).

[14] J. G. Cheng, T. Ishii, H. Kojitani, K. Matsubayashi, A. Matsuo, X. Li, Y. Shirako, J. S. Zhou, J. B. Goodenough, C. Q. Jin, M. Akaogi, and Y. Uwatoko, High-pressure synthesis of the BaIrO₃ perovskite: A Pauli paramagnetic metal with a Fermi liquid ground state, Phys. Rev. B **88**, 205114 (2013).

[15] Y. G. Shi, Y. F. Guo, Y. C. Shirako, W. Yi, X. Wang, A. A. Belik, Y. Matsushita, H. L. Feng, Y. Tsujimoto, M. Arai, N. L. Wang, M. Akaogi, and K. Yamaura, High-pressure synthesis of 5d cubic perovskite BaOsO₃ at 17 GPa: Ferromagnetic

evolution over 3d to 5d series, J. Am. Chem. Soc. **135**, 16507 (2013).

[16] J. Zhao, N. L. Ross, and R. J. Angel, New view of the high-pressure behaviour of GdFeO$_3$-type perovskites, Acta Crystallogr., Sect. B: Struct. Sci., Cryst. Eng. Mater. **60**, 263 (2004).

[17] H. J. Xiang, M. Guennou, J. Iniguez, J. Kreisel, and L. Bellaiche, Rules and mechanisms governing octahedral tilts in perovskites under pressure, Phys. Rev. B **96**, 054102 (2017).

[18] R. Vilarinho, P. Bouvier, M. Guennou, I. Peral, M. C. Weber, P. Tavares, M. Mihalik, M. Mihalik, G. Garbarino, M. Mezouar, J. Kreisel, A. Almeida, and J. A. Moreira, Crossover in the pressure evolution of elementary distortions in RFeO$_3$ perovskites and its impact on their phase transition, Phys. Rev. B **99**, 064109 (2019).

[19] G. K. Rozenberg, M. P. Pasternak, W. M. Xu, L. S. Dubrovinsky, S. Carlson, and R. D. Taylor, Consequences of pressure-instigated spin crossover in RFeO$_3$ perovskites; a volume collapse with no symmetry modification, Europhys. Lett. **71**, 228 (2005).

[20] W. M. Xu, O. Naaman, G. H. Rozenberg, M. P. Pasternak, and R. D. Taylor, Pressure-induced breakdown of a correlated system: The progressive collapse of the Mott-Hubbard state in RFeO$_3$, Phys. Rev. B **64**, 094411 (2001).

[21] V. S. Bhadram, D. Swain, R. Dhanya, M. Polentarutti, A. Sundaresan, and C. Narayana, Effect of pressure on octahedral distortions in RCrO$_3$ (R = Lu, Tb, Gd, Eu, Sm): The role of R-ion size and its implications, Mater. Res. Express **1**, 026111 (2014).

[22] J. Oliveira, J. A. Moreira, A. Almeida, V. H. Rodrigues, M. M. R. Costa, P. B. Tavares, P. Bouvier, M. Guennou, and J. Kreisel, Structural and insulator-to-metal phase transition at 50 GPa in GdMnO$_3$, Phys. Rev. B **85**, 052101 (2012).

[23] D. V. S. Muthu, A. E. Midgley, P. R. Scott, M. B. Kruger, J. R. Sahu, A. K. Sood, and C. N. R. Rao, High-pressure synchrotron x-ray diffraction study of RMnO$_3$ (R = Eu, Gd, Tb and Dy) upto 50 GPa, J. Phys. Conf. Ser. **377**, 012025 (2012).

[24] I. Loa, X. Wang, K. Syassen, H. Roth, T. Lorenz, M. Hanfland, and Y. L. Mathis, Crystal structure and the Mott-Hubbard gap in YTiO$_3$ at high pressure, J. Phys.: Condens. Matter **19**, 406223 (2007).

[25] N. L. Ross, J. Zhao, J. B. Burt, and T. D. Chaplin, Equations of state of GdFeO(3) and GdAlO(3) perovskites, J. Phys.: Condens. Matter **16**, 5721 (2004).

[26] N. L. Ross, J. Zhao, and R. J. Angel, High-pressure structural behavior of GdAlO$_3$ and GdFeO$_3$ perovskites, J. Solid State Chem. **177**, 3768 (2004).

[27] N. L. Ross, J. Zhao, and R. J. Angel, High-pressure single-crystal X-ray diffraction study of YAlO$_3$ perovskite, J. Solid State Chem. **177**, 1276 (2004).

[28] A. Senyshyn, J. M. Engel, I. D. H. Oswald, L. Vasylechko, and M. Berkowski, Powder diffraction studies of pressure-induced instabilities in orthorhombic LnGaO(3), Z Kristallogr. **2009**, 341 (2009).

[29] W. Marti, P. Fischer, F. Altorfer, H. J. Scheel, and M. Tadin, Crystal-Structures and Phase-Transitions of Orthorhombic and Rhombohedral (RGaO$_3$ R = La, Pr, Nd) Investigated by Neutron Powder Diffraction, J. Phys.: Condens. Matter **6**, 127 (1994).

[30] M. Ardit, G. Cruciani, M. Dondi, M. Merlini, and P. Bouvier, Elastic properties of perovskite YCrO$_3$ up to 60 GPa, Phys. Rev. B **82**, 064109 (2010).

[31] R. J. Angel, J. Zhao, N. L. Ross, C. Jakeways, S. A. T. Redfern, and M. Berkowski, High-pressure structural evolution of a perovskite solid solution (La$_{1-x}$, Nd$_x$)GaO$_3$, J. Solid State Chem. **180**, 3408 (2007).

[32] M. Amboage, M. Hanfland, J. A. Alonso, and M. J. Martinez-Lope, High pressure structural study of SmNiO$_3$, J. Phys.: Condens. Matter **17**, S783 (2005).

[33] I. Loa, P. Adler, A. Grzechnik, K. Syassen, U. Schwarz, M. Hanfland, G. K. Rozenberg, P. Gorodetsky, and M. P. Pasternak, Pressure-Induced Quenching of the Jahn-Teller Distortion and Insulator-To-Metal Transition in LaMnO$_3$, Phys. Rev. Lett. **87**, 125501 (2001).

[34] J. S. Zhou, J. B. Goodenough, and B. Dabrowski, Structure anomaly and electronic transition in RNiO$_3$ (R = La,Pr, …,Gd), Phys. Rev. B **70**, 081102(R) (2004).

[35] See Supplemental Material at http://link.aps.org/supplemental/10.1103/PhysRevB.101.224104 for additional information about refinement details and the data of high-pressure structural study on RMO$_3$.

[36] M. O' Keeffe and B. G. Hyde, Some Structures Topologically Related to Cubic Perovskite ($E2_1$), ReO$_3$ (Do_9) and Cu$_3$Au($L1_2$), Acta Crystallogr., Sect. B: Struct. Sci., Cryst. Eng. Mater. **33**, 3802 (1977).

[37] M. W. Lufaso and P. M. Woodward, Prediction of the crystal structures of perovskites using the software program $SPuDS$, Acta Crystallogr., Sect. B: Struct. Sci., Cryst. Eng. Mater. **57**, 725 (2001).

[38] M. W. Lufaso, P. W. Barnes, and P. M. Woodward, Structure prediction of ordered and disordered multiple octahedral cation perovskites using SPuDS, Acta Crystallogr., Sect. B: Struct. Sci., Cryst. Eng. Mater. **62**, 397 (2006).

[39] J. S. Zhou and J. B. Goodenough, Universal Octahedral-Site Distortion in Orthorhombic Perovskite Oxides, Phys. Rev. Lett. **94**, 065501 (2005).

[40] K. Oikawa, T. Kamiyama, T. Hashimoto, Y. Shimojyo, and Y. Morii, Structural phase transition of orthorhombic LaCrO$_3$ studied by neutron powder diffraction, J. Solid State Chem. **154**, 524 (2000).

[41] J. S. Zhou, J. A. Alonso, A. Muonz, M. T. Fernandez-Diaz, and J. B. Goodenough, Magnetic Structure of LaCrO$_3$ Perovskite under High Pressure from In Situ Neutron Diffraction, Phys. Rev. Lett. **106**, 057201 (2011).

[42] T. Shibasaki, T. Furuya, J. Kuwahara, Y. Takahashi, H. Takahashi, and T. Hashimoto, Exploration of high pressure phase in LaGaO$_3$ and LaCrO$_3$, J. Therm. Anal. Calorim. **81**, 575 (2005).

[43] P. W. Anderson, New approach to the theory of superexchange interactions, Phys. Rev. **115**, 2 (1959).

[44] J. S. Zhou and J. B. Goodenough, Intrinsic structural distortion in orthorhombic perovskite oxides, Phys. Rev. B **77**, 132104 (2008).

[45] J. S. Zhou and J. B. Goodenough, Pressure-Induced Transition from Localized Electron Toward Band Antiferromagnetism in LaMnO$_3$, Phys. Rev. Lett. **89**, 087201 (2002).

[46] F. Aguado, F. Rodriguez, and P. Nunez, Pressure-induced Jahn-Teller suppression and simultaneous high-spin to low-spin

transition in the layered perovskite CsMnF$_4$, Phys. Rev. B. **76**, 094417 (2007).

[47] M. N. Sanz-Ortiz and F. Rodriguez, Photoluminescence properties of Jahn-Teller transition-metal ions, J. Chem. Phys. **131**, 124512 (2009).

[48] J. Kanamori, Crystal Distortion in Magnetic Compounds, J. Appl. Phys. **31**, S14 (1960).

[49] J. S. Zhou and J. B. Goodenough, Unusual Evolution of the Magnetic Interactions Versus Structural Distortions in RMnO$_3$ Perovskites, Phys. Rev. Lett. **96**, 247202 (2006).

[50] T. Hashimoto, N. Matsushita, Y. Murakami, N. Kojima, K. Yoshida, H. Tagawa, M. Dokiya, and T. Kikegawa, Pressure-induced structural phase transition of LaCrO$_3$, Solid State Commun. **108**, 691 (1998).

[51] B. J. Kennedy, T. Vogt, C. D. Martin, J. B. Parise, and J. A. Hriljac, Pressure-induced orthorhombic to rhombohedral phase transition in LaGaO$_3$, J. Phys.: Condens. Matter **13**, L925 (2001).

[52] M. Medarde, J. Mesot, S. Rosenkranz, P. Lacorre, W. Marshall, S. Klotz, J. S. Loveday, G. Hamel, S. Hull, and P. Radaelli, Pressure-induced orthorhombic-rhombohedral phase transition in NdNiO$_3$, Physica B (Amsterdam, Neth.) **234**, 15 (1997).

[53] O. L. Anderson and N. Soga, A Restriction to Law of Corresponding States, J. Geophys. Res. **72**, 5754 (1967).

[54] D. L. Anderson and O. L. Anderson, Bulk Modulus-Volume Relationship for Oxides, J. Geophys. Res. **75**, 3494 (1970).